

- [2] M. Böltau, S. Walheim, J. Mlynek, G. Krausch, U. Steiner, *Nature* **1998**, 391, 877.
- [3] G. Krausch, E. J. Kramer, M. H. Rafailovich, J. Sokolov, *Appl. Phys. Lett.* **1994**, 64, 2655.
- [4] A. Arias, N. Corcoran, M. Banach, R. H. Friend, W. T. S. Huck, *Appl. Phys. Lett.* **2002**, 80, 1695.
- [5] A. C. Arias, J. D. Mackenzie, R. Stevenson, J. J. M. Halls, M. Inbasekaran, E. P. Woo, D. Richards, R. H. Friend, *Macromolecules* **2001**, 34, 6005.
- [6] J. J. M. Halls, A. C. Arias, J. D. Mackenzie, M. Inbasekaran, E. P. Woo, R. H. Friend, *Adv. Mater.* **2000**, 12, 498.
- [7] J.-S. Kim, P. K. H. Ho, N. C. Greenham, R. H. Friend, *J. Appl. Phys.* **2000**, 88, 1073.
- [8] B. J. Matterson, J. M. Lupton, A. F. Safonov, M. G. Salt, W. L. Barnes, I. D. W. Samuel, *Adv. Mater.* **2001**, 13, 123.
- [9] J. R. Lawrence, P. Andrew, W. L. Barnes, M. Buck, G. A. Turnbull, I. D. W. Samuel, *Appl. Phys. Lett.* **2002**, 81, 1955.
- [10] S. Fan, R. Villeneuve, J. D. Joannopoulos, E. F. Schubert, *Phys. Rev. Lett.* **1997**, 78, 3294.
- [11] M. Boroditsky, T. F. Krauss, R. Coccioli, R. Vrijen, R. Bhat, E. Yablonovitch, *Appl. Phys. Lett.* **1999**, 75, 1036.
- [12] A. Budkowski, A. Bernasik, P. Cyganik, J. Rysz, R. Brenn, *E-Polymers* **2002**, No. 6.
- [13] J. Morgado, E. Moons, R. H. Friend, F. Cacialli, *Synth. Met.* **2001**, 124, 63.
- [14] A. W. Grice, D. D. C. Bradley, M. T. Bernius, M. Inbasekaran, W. W. Wu, E. P. Wo, *Appl. Phys. Lett.* **1998**, 73, 629.
- [15] R. Stevenson, A. C. Arias, C. Ramsdale, J. D. Mackenzie, D. Richards, *Appl. Phys. Lett.* **2001**, 79, 2178.
- [16] D. A. G. Bruggeman, *Ann. Phys.* **1935**, 24, 636.
- [17] S. Walheim, M. Böltau, J. Mlynek, G. Krausch, U. Steiner, *Macromolecules* **1997**, 30, 4995.

## Color Micro- and Nanopatterning with Counter-Propagating Reaction–Diffusion Fronts\*\*

By Christopher J. Campbell, Marcin Fialkowski, Rafal Klajn, Igor T. Bensemann, and Bartosz A. Grzybowski\*

Competition between reaction and diffusion (RD) can lead to the emergence of intricate spatial and/or temporal patterns<sup>[1–3]</sup> in both chemical<sup>[4,5]</sup> and biological systems.<sup>[6,7]</sup> Phenomena as diverse as oscillating reactions,<sup>[8]</sup> periodic precipi-

tation fronts,<sup>[9,10]</sup> chemical turbulence via catalytic reactions,<sup>[11]</sup> cardiac waves,<sup>[12]</sup> and formation of bacterial colonies of regular morphologies,<sup>[13]</sup> are all manifestations of the subtle interplay between interconversion (i.e., reaction) of participating chemicals and their diffusion. While nature often uses RD as a means of making structures and materials of unique properties or morphologies on scales ranging from macro- (e.g., stripes in zebras, tigers, and seashells, and formations in trees, agates, and rocks)<sup>[7,14,15]</sup> to microscopic (e.g., cellular growth,<sup>[16]</sup> chemotaxis,<sup>[17]</sup> and biological waves<sup>[18]</sup>), reaction–diffusion phenomena have not yet been applied in modern material science and microtechnology. In this context, RD systems are particularly promising for the micropatterning of surfaces.<sup>[19,20]</sup> Unlike conventional micropatterning techniques that modify the properties of the substrate only at the locations to which a modifying agent—be it a chemical<sup>[21,22]</sup> or radiation<sup>[23,24]</sup>—is delivered, RD can, in principle, evolve chemicals delivered onto a surface into structures of characteristic dimensions significantly smaller than those of the original pattern. Here, we describe an experimental system in which reaction–diffusion transforms microscopic patterns of chemicals delivered onto thin films of dry gelatin into regular arrays of lines of submicrometer thicknesses.

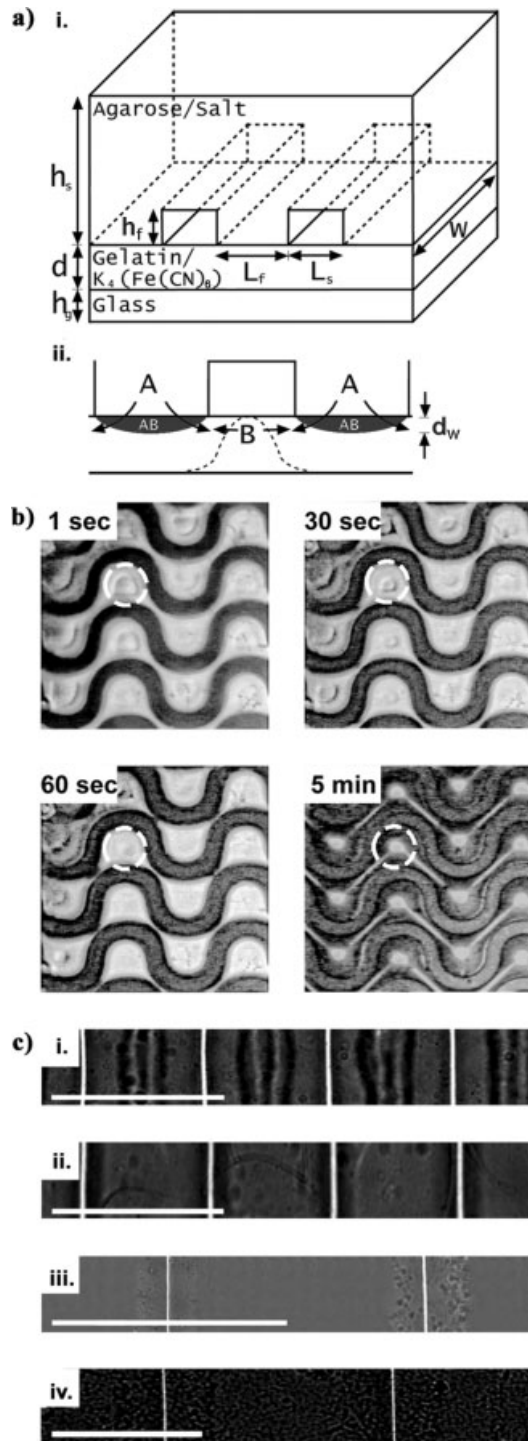
In this system, the gel is doped with potassium hexacyanoferrate(II),  $K_4Fe(CN)_6$ , and a solution of an inorganic salt is delivered onto its surface from an agarose stamp patterned in bas-relief. When the salt diffuses from the stamp into the gel, its metal cations react with  $[Fe(CN)_6]^{4-}$  to give a deeply colored precipitate. Remarkably, production of the precipitate decreases the diffusion coefficient of hexacyanoferrate ions to a greater effect than the diffusion coefficient of the cations delivered from the stamp. This selective decrease causes reaction fronts originating from different features of the stamp to slow down exponentially as they approach one another. When these fronts ultimately come to a halt, they leave a sharp, clear region in between. The characteristic dimensions of this region are up to two orders of magnitude smaller than the spacing between the features in the agarose stamp, and can be controlled by the concentrations of the chemicals used and/or by the spacing between the features.

Figure 1a illustrates the procedure. An agarose stamp (8 % w/w OmniPur Agarose, Darmstadt, Germany,) patterned in bas-relief and soaked in a solution of an inorganic salt (typically iron(III) chloride, cobalt(II) chloride, or copper(II) chloride, 0.1–2.0 M) is brought into conformal contact with a thin layer of dry gelatin doped with 0.5–5 wt.-% of potassium hexacyanoferrate,  $K_4Fe(CN)_6$ . The salts in the stamp are chosen in such a way that their cations react with  $[Fe(CN)_6]^{4-}$  to give deeply colored precipitates. For example,  $FeCl_3$  gives a dark-blue precipitate (Prussian Blue),  $CoCl_2$ —turquoise, and  $CuCl_2$ —brown.

Water from the stamp rapidly wets the surface of dry gelatin and slowly diffuses into its bulk. Wetting of the surface is driven by capillarity and occurs at a rate of  $\sim 1.5 \mu m s^{-1}$ ; the transport of water into the bulk of the gel is a diffusive process against the osmotic pressure due to the immobilized

[\*] Prof. B. A. Grzybowski, C. J. Campbell, Dr. M. Fialkowski, R. Klajn, Dr. I. T. Bensemann  
Department of Chemical and Biological Engineering  
Northwestern University  
2145 Sheridan Rd, Evanston, IL 60208 (USA)  
E-mail: grzybor@northwestern.edu

[\*\*] B. A. G. gratefully acknowledges financial support from Northwestern University start-up funds and from the Camille and Henry Dreyfus New Faculty Awards Program. C. J. C. was supported in part by the NSF-IGERT program “Dynamics of Complex Systems in Science and Engineering” (DGE-9987577). M. F. was supported by the NATO Post-Graduate Scientific Fellowship Program.



**Figure 1.** Wet-stamping procedure. a) i. Illustrates the experimental set-up for patterning salt solutions onto thin films of dry gelatin, and defines the pertinent dimensions:  $d = 30\text{--}50\ \mu\text{m}$ ,  $L_s = 25\text{--}250\ \mu\text{m}$ ,  $L_f = 50\text{--}250\ \mu\text{m}$ ,  $h_s = 0.5\text{--}2\ \text{cm}$ ,  $h_f \sim 50\ \mu\text{m}$ ,  $h_g = 1\ \text{mm}$ ,  $w = 1\ \text{cm}$ . ii. A qualitative description of the reaction-diffusion processes inside of a patterned gel. b) Upon stamping, water rapidly wets the gelatin film; reaction (color) front moves much slower than the swelling front (denoted by white dotted circles). c) Sub-micrometer lines from experiments with different salts. The line widths are i. 950 nm (1.25 M  $\text{CoCl}_2$ ) ii. 910 nm (1.0 M  $\text{CuCl}_2$ ) iii. 300 nm (1.0 M  $\text{FeCl}_3$ ) iv. 490 nm (0.29 M  $\text{CuCl}_2$ /0.39 M  $\text{CoCl}_2$ ) Scale bars are 100  $\mu\text{m}$ ; for true colors of the salts see Figure 3.

$\text{K}_4\text{Fe}(\text{CN})_6$ , and is characterized by the diffusion coefficient  $D_w \sim 10^{-7}\ \text{cm}^2\ \text{s}^{-1}$ .<sup>[25]</sup> When the metal cations carried by water enter the gel, they are instantaneously precipitated in reaction with  $[\text{Fe}(\text{CN})_6]^{4-}$ . Their local concentration is replenished by more cations supplied from the stamp, but the reaction (i.e., color) front does not propagate until all hexacyanoferrate ions at a given location are used. As a result, the reaction front travels slower (effective diffusion constant in the plane of the surface,  $D_s \sim 10^{-5}\ \text{cm}^2\ \text{s}^{-1}$ ) than water swelling the gelatin (Fig. 1b). In other words, metal cations entering the gel diffuse and react within a thin layer of an already swollen gel near the surface. The thickness of this layer,  $d_w$ , can be estimated from the relation  $d_w \sim \sqrt{D_w/D_s} \cdot L_s$ , where  $L_s$  is a characteristic distance the reaction front travels (typically, tens of micrometers); with the measured values of the diffusion coefficients,  $d_w$  is on the order of several micrometers.

As the cations constantly delivered from the stamp migrate through the gel, they precipitate all  $[\text{Fe}(\text{CN})_6]^{4-}$  they encounter. The unreacted hexacyanoferrate ions experience a sharp concentration gradient at the reaction front, and diffuse in its direction. In case of two reaction fronts counter-propagating from nearby features of the stamp, hexacyanoferrate ions between them diffuse outwards, towards the incoming fronts (Fig. 1a, lower picture). This outflow continues until, ultimately, there is no more  $[\text{Fe}(\text{CN})_6]^{4-}$  left near the centerline between the features. Although the cations continue to diffuse into this region, there are no more  $[\text{Fe}(\text{CN})_6]^{4-}$  ions left to precipitate, and the region remains a thin, uncolored line of well defined boundaries and a typical thickness of one to two orders of magnitude smaller than the spacing between the neighboring features in the stamp (Fig. 1c).

The appearance of sharp, clear lines cannot be explained without accounting for the dependence of the diffusion coefficients of the participating salts on both the spatial location and on the concentration of the precipitate. We have recently shown<sup>[25]</sup> that the amount of water absorbed by a thin film of dry gelatin doped with potassium hexacyanoferrate (or another inorganic salt) decreases exponentially with the distance from the surface to which water was delivered. Consequently, diffusion coefficients of the species migrating in such a non-uniformly swollen, ionic gel decrease rapidly with depth. Furthermore, we found that for the salt/ $\text{K}_4\text{Fe}(\text{CN})_6$  system studied here, diffusion coefficient of the migrating  $[\text{Fe}(\text{CN})_6]^{4-}$  ions decreases with increasing amount of the precipitate, while that of the metal cations is not affected by precipitation (see Experimental and Methods).

Based on these observations, we developed a theoretical model that explains the formation of color patterns in our system. Let  $A$  be the concentration of the metal cations delivered to the gel (typically, 0.5 M),  $B$  the concentration of  $[\text{Fe}(\text{CN})_6]^{4-}$  in the swollen gel (about 0.25 M), and  $C$  the concentration of the precipitate. The rate constant for precipitation is denoted as  $k$ , the solubility product as  $K_{\text{sp}}$ , and  $D_{A,B}$  are the diffusion coefficients of  $A$  and  $B$ , respectively. We consider a quasi two-dimensional geometry of an array of infinite, parallel lines (of thickness  $L_f$  and spaced by  $L_s$ ) stamped onto

gelatin. The process of transferring *A* from these lines into a dry gel containing *B* is described by a system of reaction-diffusion partial differential equations. For the reaction of the type  $nA + mB \rightarrow C \downarrow$  (*n* and *m* are the stoichiometric coefficients) and in dimensionless variables (with time *t* measured in units of  $L_f^2/D_A$  and spatial variables *x* and *y* are measured in units of  $L_f$ ), the RD equations take the following form:

$$\partial A / \partial \tau = D_A^{-1} \nabla D_A \nabla A - \delta_A \theta(A^n B^m - K_{sp}) \quad (1)$$

$$\partial B / \partial \tau = D_B^{-1} \nabla D_B \nabla B - \delta_B \theta(A^n B^m - K_{sp}) \quad (2)$$

$$\partial C / \partial \tau = \delta_C \theta(A^n B^m - K_{sp}) \quad (3)$$

where  $K_{sp} = (A - \delta_A)^n (B - m\delta_A/n)^m$ ,  $\delta_B = n\delta_A/m$  and  $\delta_C = \delta_A/n$ , and the Heaviside step function  $\theta$  accounts for the fact that the precipitation reaction is much faster than the transport of components.<sup>[26]</sup> The values of diffusion coefficients depend on the distance from the surface of the gel, and on the concentration of the precipitate:  $D_A(y) = D_A^0 \eta(y)$ , and  $D_B(x,y) = D_B^0 \eta(y) \exp[-\alpha C(x,y)]$ , where  $\alpha$  is a constant and  $\eta(y) = 1$  for  $d > y > d - d_w$  and 0 otherwise. With these assumptions, and imposing periodic boundary conditions, the RD equations can be solved numerically to give concentration (i.e., color) profiles of the precipitate.

The results of numerical simulations agree with experiment. Figure 2b compares the experimental color profiles with the calculated concentration profiles of the precipitate (Prussian Blue) for a  $\text{FeCl}_3/\text{K}_4\text{Fe}(\text{CN})_6$  system ( $n = 4$ ,  $m = 3$ ,  $A_0 = 1.0$  M,  $B_0 = 0.25$  M,  $K_{sp} = 3.3 \times 10^{-41}$ ,  $d_w = 8 \mu\text{m}$ ,  $L_f = 50 \mu\text{m}$ ,  $L_s = 150 \mu\text{m}$ ,  $D_B^0/D_A^0 = 0.3$ , and  $\alpha = 10 \text{ M}^{-1}$ ). The model predicts that the concentration of *C* – and thus the intensity of the blue color – initially increases slowly with distance from the edge of the stamped line, and then rapidly drops to less than 1 % of the maximum value – this sharp minimum corresponds to the clear line observed in experiments. The width of the line,  $L_{cl}$ , is  $1.81 \pm 0.24 \mu\text{m}$  in experiments and  $2.39 \mu\text{m}$  according to the model. The value of  $L_{cl}$  scales approximately linearly with  $L_s$  (with the constant of proportionality  $\beta \sim 0.01$ ; Fig. 2c), and with the concentration of  $\text{FeCl}_3$  over the range of concentrations from 0.1 M up to 2 M ( $dL_{cl}/d[\text{FeCl}_3] = \gamma$ ;  $\gamma \sim -1 \mu\text{m M}^{-1}$  in experiment and  $\gamma \sim -0.6 \mu\text{m M}^{-1}$  in the model). Qualitatively similar, linear trends hold for  $\text{CuCl}_2/\text{K}_4\text{Fe}(\text{CN})_6$  and  $\text{CoCl}_2/\text{K}_4\text{Fe}(\text{CN})_6$  systems we studied, but the values of the  $\beta$  and  $\gamma$  coefficients are about twice as high as those for  $\text{FeCl}_3/\text{K}_4\text{Fe}(\text{CN})_6$ .

When arrays other than those of parallel lines are stamped, they develop into patterns that are often very intricate and sometimes even counter-intuitive (Fig. 3). For example, wavy lines generate straight lines (Figs. 3a,1b); crosses develop into 14-sided polygons (Fig. 3b); widely separated squares give square-circle-square arrays (Fig. 3c); snaking lines evolve into curvy lines (Fig. 3d), and arrays of circles of different sizes give space-filling patterns with two types of curvilinear tiles (Fig. 3e). The technique allows developing these patterns

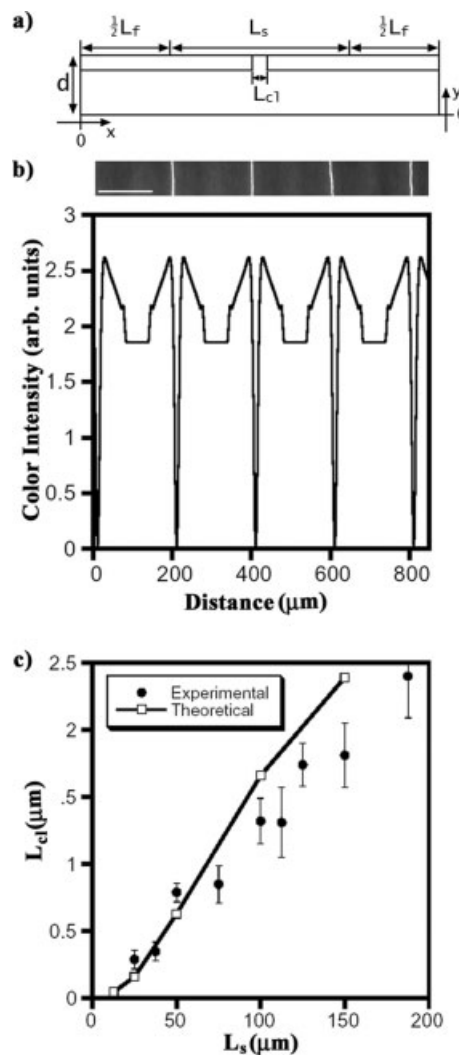


**Figure 2.** Experimental and theoretical color profiles from 1 M  $\text{FeCl}_3$ . a) The coordinates and spatial variables used in calculations ( $L_{cl}$  is the width of the developed clear line between the stamped features.) b) Upper picture is an optical micrograph of a pattern obtained by stamping an array of parallel lines ( $L_f = 50 \mu\text{m}$ ,  $L_s = 100 \mu\text{m}$ ); scale bar is  $100 \mu\text{m}$ . The graph below is the calculated profile of the intensity of the blue color in the gelatin film for the values of parameters same as those used in the experiment. c) Theoretical (open markers) and experimental (closed markers) dependence of  $L_{cl}$  on  $L_s$ .

into either the final, steady state, or only to a certain degree. For example, wavy lines can be evolved into fully developed zig-zags (Fig. 1b), or into patterns in which diagonal straight lines are interspersed with “windows”—that is, regions where the fronts are still far away from each other at the time the lines form (Fig. 3a). Although we were able to reproduce all of these patterns using the RD equations, these calculations were very time consuming. For practical and efficient modeling, we developed a heuristic, geometrical algorithm<sup>[27]</sup> that is based on the minimization of Hausdorff’s distances<sup>[28]</sup> between the stamped features, and that correctly predicts the morphologies of patterns (Fig. 3 g,h).

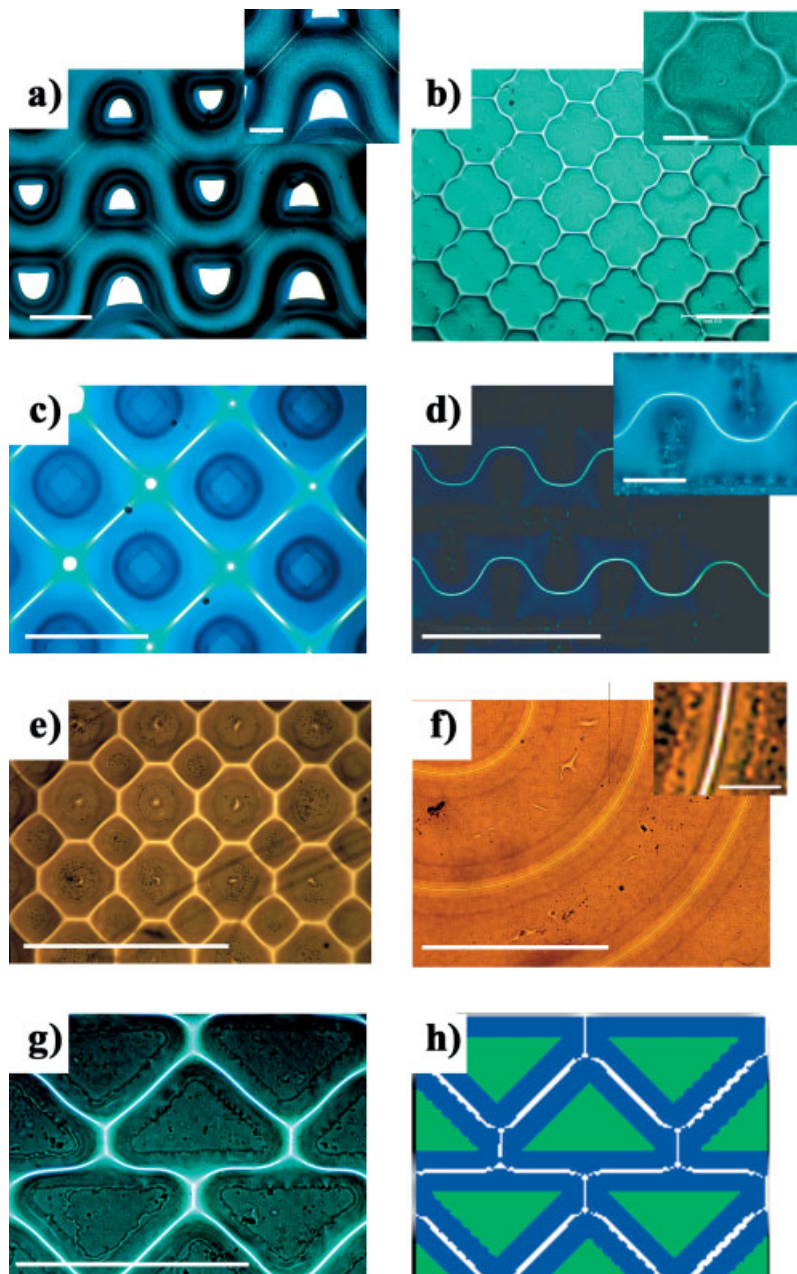


**Figure 3.** Curvilinear color patterns a) Wavy lines not completely developed, leaving uncolored “windows” between diagonal lines (0.75 M FeCl<sub>3</sub>). b) Pattern emerging from an array of crosses (0.75 M CoCl<sub>2</sub>). c) Pattern developed from an array of squares separated by large distances ( $L_s=150\ \mu\text{m}$ ,  $L_f=50\ \mu\text{m}$ , 1 M FeCl<sub>3</sub>) d) Array of snaking lines evolved from a stamp (0.75 M FeCl<sub>3</sub>) having an array of interdigitated lines embossed on its surface. e) Space-filling tiling obtained from an array of circles of two sizes (50  $\mu\text{m}$  and 100  $\mu\text{m}$ , 1.0 M CuCl<sub>2</sub>). f) Array of clear, concentric circles (~750 nm wide) developed from a pattern of concentric rings (75  $\mu\text{m}$  thick spaced by 75  $\mu\text{m}$ ; 1.0 M CuCl<sub>2</sub>). Experimental (0.75 M CoCl<sub>2</sub>) g) and calculated h) patterns obtained from an array of triangles. Scale bars are 250  $\mu\text{m}$ ; insert scale bars in (a,b,d) are 100  $\mu\text{m}$ ; in (f) 5  $\mu\text{m}$ .

To illustrate the applicability of our method, we used the color-patterned gels as high-quality diffraction gratings (Fig. 4a,b) and photolithographic masks (Fig. 4c). When used as masks, the colored portions of the films prepared with concentrated (1 M) FeCl<sub>3</sub> were completely opaque to UV radia-

tion, and the developed photoresist had binary topography. In contrast, for less concentrated salts - especially in the CoCl<sub>2</sub>/K<sub>4</sub>Fe(CN)<sub>6</sub> system—the intensity of transmitted radiation reflected the concentration gradient of the turquoise precipitate in the stamp, and the developed photoresist had a continuously varying topography. Gradient photomasks could also be prepared by using a variant of our method, in which the stamp was soaked in a mixture of two salts of different diffusivities and solubility products with respect to [Fe(CN)<sub>6</sub>]<sup>4-</sup> ions. For appropriate ratio of concentrations in the stamp, the precipitates of different salts (and colors) formed at different regions of the film (Fig. 4d); these regions had different optical transmissivities.

The method we described offers a versatile approach to submicrometer color patterning of surfaces. In addition to being a method to generate diffraction gratings and photolithographic masks, we envision its further possible uses in fabrication of arrays of planar wave-guides (in systems, in which the precipitate and the salt solutions would have sufficiently different indices of refraction), and in sensory/assay applications in which the thickness of the clear lines would provide a direct readout of the concentrations/mobilities of chemicals (or biomolecules) reacting and diffusing in the gel. Finally, we suggest that the method could be of use in topology as a practical way of determining space-filling tilings of complex shapes (cf. Fig. 3b,e).

### Experimental and Methods

*Dry Versus Wet Gelatin Surfaces:* Dry instead of wet gels were used, because in the latter water initially migrated from the gelatin into the stamp to equalize the osmotic pressures. This backflow resulted in the deformation of the gelatin surface and the loss of conformal contact. In addition, when osmotic pressures ultimately equalized and salts diffused from agarose into wet gelatin, they penetrated to a much deeper depth than when dry gelatin was used. As observed in experiments and confirmed by simulations, this deep penetration reduced the optical contrast between colored and clear regions of the final patterns.

*Diffusion Coefficients:* i) The effect of precipitation on the diffusion coefficients of migrating ions was established in a series of experiments in which solutions of K<sub>4</sub>Fe(CN)<sub>6</sub> and one of the salts (i.e., FeCl<sub>3</sub>, CoCl<sub>2</sub> or CuCl<sub>2</sub>) diffused towards each other from the opposite ends of a glass tube filled with wet gelatin. When diffusion fronts met, they gave a colored precipitate. Subsequently, the front of the colored zone propagated only towards the source of [Fe(CN)<sub>6</sub>]<sup>4-</sup>, indicating that the precipitate inhibited the diffusion of [Fe(CN)<sub>6</sub>]<sup>4-</sup> ions towards the source of the other salt. ii) The ratio of

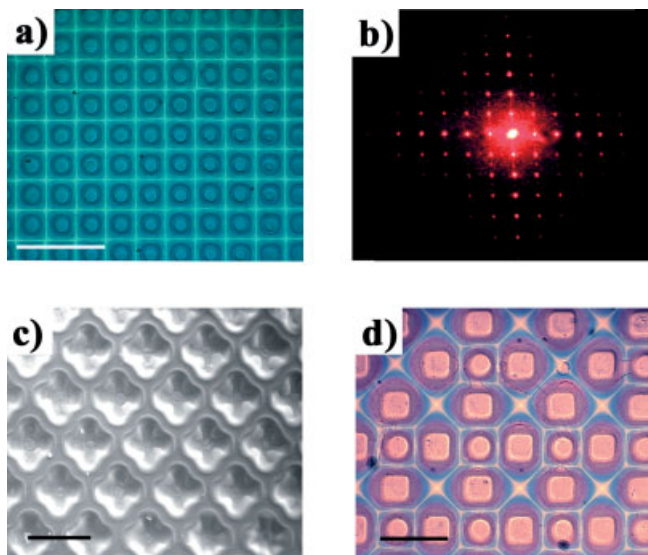


**Figure 4.** Applications and extensions of the color-patterning method. a) Shows a square array of  $\sim 4 \mu\text{m}$  thick, clear lines obtained by stamping a pattern of  $50 \mu\text{m}$  circles spaced by  $50 \mu\text{m}$ . This array was used as a diffraction grating that upon irradiation with  $632 \text{ nm}$  laser produced a diffraction pattern shown in b). c) An array of crosses (same as in Fig. 3b) stamped from  $0.75 \text{ M CoCl}_2$  is used as a photolithographic mask (UV exposure on silicon wafer spin-coated with  $50 \mu\text{m}$  of SU-8 50 photoresist). The quasi three-dimensional topography of the developed pattern reflects the gradient of color intensity in the stamped gel. d) Two-color pattern obtained by using a stamp soaked in a mixture of  $\text{FeCl}_3$  and  $\text{CuCl}_2$  ( $0.5 \text{ M}$  each). Separation of colors is a result of a subtle interplay between the diffusion coefficients and solubility products of the two salts. Although the solubility product (with respect to  $[\text{Fe}(\text{CN})_6]^{4-}$ ) of  $\text{Fe}^{3+}$  is lower than that of  $\text{Cu}^{2+}$ , copper cations diffuse into gelatin more rapidly than iron cations—consequently, they react with  $[\text{Fe}(\text{CN})_6]^{4-}$  first, and give a layer of brown precipitate under and in the vicinity of every stamped feature. The iron cations supplied from the stamp enter a zone already depleted of  $[\text{Fe}(\text{CN})_6]^{4-}$  and must diffuse outwards in order to precipitate. Since the local concentration of  $\text{Fe}^{3+}$  is higher than that of the depleted  $\text{Cu}^{2+}$  (which is being slowly re-supplied from the stamp), iron cations migrate outwards more rapidly (despite having lower coefficient of diffusion) than copper cations; ultimately, they form a zone of a blue precipitate around every brown region. All scale bars are  $300 \mu\text{m}$ .

the salts' diffusion coefficients,  $D_B^0/D_A^0$  was estimated in an experiment in which two agarose blocks soaked in  $\text{FeCl}_3$  and  $\text{K}_4(\text{Fe}(\text{CN})_6)$  respectively, were placed about  $0.5 \text{ cm}$  apart on a film of pure, dry gelatin. The salts diffused towards each other, and when they met they precipitated along a line parallel to the edges of the blocks. The ratio  $D_B^0/D_A^0$  was equal to the ratio of squares of distances from the edges of the stamps to the precipitation line.

**Modeling Details:** The RD model assumed the concentration of the salt in the stamp to be constant, and the upper and lower boundaries of the gel layer to be closed with respect to the diffusion of the internal ions. The use of Heaviside step functions allowed the separation of time scales for diffusion (slow) and precipitation (very fast) [26]; it implied that if the concentrations of ions was above  $K_{sp}$ , precipitation occurred instantaneously.

The RD equations were solved numerically using the Crank–Nicolson integration scheme and with the following initial-boundary conditions: i) for the metal cations:  $A(x,y,t) = A_0$  at the stamp–gel interface ( $y = d$  and  $0 < x < L_f/2$  and  $L_s + L_f/2 < x < L_s + L_f$ ) and  $\nabla A(x,y) = 0$  for  $y = d$  and  $L_f/2 < x < L_s + L_f/2$  and for  $y = 0$ ; ii) for the hexacyanoferrate ions and the precipitate:  $B(x,y,\tau = 0) = B_0$ ;  $C(x,y,\tau = 0) = 0$ ; and  $\nabla B(x,y) = 0$  for  $y = 0, d$ . To account for the infinite size of the gel in the  $x$  direction, periodic boundary conditions on the

concentrations of  $A$ ,  $B$ , and  $C$  were imposed in the  $x$  direction. The diffusion coefficients were assumed to have the following forms:  $D_A(y) = D_A^0 \eta(y)$ , and  $D_B(x,y) = D_B^0 \eta(y) \exp[-\alpha C(x,y)]$ , where  $\alpha$  was a constant. The function  $\eta(y) = 1$  for  $d > y > d - d_w$ , and 0 otherwise accounted for the fact that the ions diffused only within a thin, wetted surface layer of thickness  $d_w$ . The exponential term reflected the decrease of the diffusion coefficient with the increase of the concentration of the precipitate  $C(x,y)$ ; exponential dependence of this type has been previously shown to be suitable to describe the diffusion of small particles in multicomponent systems [29,30]. The input parameters in the simulations were the initial concentrations  $A_0$ , and  $B_0$ , and the ratio of diffusion coefficients. Parameter  $\alpha$  was fitted such as to minimize the amount of precipitate in the centerline region; the value used to generate Figure 2b was  $10 \text{ M}^{-1}$  and was used in all subsequent calculations (the results of the simulations did not differ perceptibly with the value of  $\alpha$  changing up to 20 %).

The theoretical widths of the clear lines were measured at 5 % of the maximal height of the integrated concentration of the precipitate. As verified experimentally, this value corresponded to a threshold below which the gel could be considered transparent.

Received: March 12, 2004

Final version: May 15, 2004

Published online: October 14, 2004

- [1] A. M. Turing, *Philos. Trans. R. Soc. London* **1952**, 237, 37.
- [2] G. Nicolis, I. Prigogine, *Self-organization in Nonequilibrium Systems – From Dissipative Structures to Order through Fluctuations*, Wiley, New York **1977**.
- [3] A. M. Zhabotinsky, A. N. Zaikin, *Nature* **1970**, 225, 535.
- [4] I. Lengyel, I. R. Epstein, *Science* **1991**, 251, 650.
- [5] Q. Ouyang, H. L. Swinney, *Nature* **1991**, 352, 610.
- [6] B. Hess, A. Mikhailov, *Science* **1994**, 264, 223.
- [7] D. Thompson, *On Growth and Form*, Cambridge University Press, Cambridge, UK **1992**.
- [8] A. M. Zhabotinsky, M. Dolnik, I. R. Epstein, *J. Chem. Phys.* **1995**, 103, 10306.
- [9] H. K. Henisch, *Crystals in Gels and Liesegang Rings*, Cambridge University Press, Cambridge, UK **1998**.
- [10] S. C. Müller, J. Ross, *J. Phys. Chem. A* **2003**, 107, 7997.
- [11] G. Ertl, *Science* **1991**, 254, 1750.
- [12] R. A. Gray, A. M. Pertsov, J. Jalife, *Nature* **1998**, 392, 75.
- [13] J. A. Shapiro, D. Trubatch, *Phys. D (Amsterdam, Neth.)* **1991**, 49, 214.
- [14] H. Meinhardt, *Models of Biological Pattern Formation*, Academic Press, London **1982**.
- [15] P. Ball, *Self-Made Tapestry: Pattern Formation in Nature*, Oxford University Press, Oxford, UK **2001**.
- [16] J. D. Murray, in *The Handbook of Brain Theory and Neural Networks* (Ed. M. A. Arbib), MIT Press, Cambridge, MA **2003**, p. 851.
- [17] R. Tyson, S. R. Lubkin, J. D. Murray, *Proc. R. Soc. London, Ser. B* **1998**, 299, 299.
- [18] A. Kolmogoroff, I. Petrovsky, N. Piscounoff, *Moscow Univ. Math. Bull. (Engl. Transl.)* **1937**, 1, 1.
- [19] P. R. Choudhury, *Handbook of Microlithography, Micromachining, & Microfabrication*, SPIE, Bellingham, WA **1997**.
- [20] B. Michel, A. Bernard, A. Bietsch, E. Delamarche, M. Geissler, D. Juncker, H. Kind, J.-P. Renault, H. Rothuizen, H. Schmid, P. Schmidt-Winkel, R. Stutz, H. Wolf, *IBM J. Res. Dev.* **2001**, 45, 697.
- [21] E. Delamarche, C. Donzel, F. S. Kamounah, H. Wolf, M. Geissler, R. Stutz, P. Schmidt-Winkel, B. Michel, H. J. Mathieu, K. Schaumburg, *Langmuir* **2003**, 19, 8749.
- [22] Y. Xia, G. M. Whitesides, *Angew. Chem. Int. Ed.* **1998**, 37, 551.
- [23] D. W. L. Tolfree, *Rep. Prog. Phys.* **1998**, 61, 313.
- [24] L. F. Thompson, R. E. Kerwin, *Ann. Rev. Mater. Sci.* **1976**, 6, 267.

- [25] M. Fialkowski, C. J. Campbell, I. T. Bensemann, B. A. Grzybowski, *Langmuir* **2004**, *20*, 3513.
- [26] I. V. Tananayez, M. A. Glushkova, B. G. Seifer, *Zh. Neorg. Khim.* **1956**, *1*, 66.
- [27] The executable program for the algorithm, along with instructions, can be found at <http://dysa.northwestern.edu/programs/patternfinder.html>
- [28] B. Gruenbaum, G. C. Shephard, *Tilings and Patterns*, W. H. Freeman, New York **1987**.
- [29] P. Gao, P. E. Fagerness, *Pharm. Res.* **1995**, *12*, 955.
- [30] L. Masaro, X. X. Zhu, *Prog. Polym. Sci.* **1995**, *20*, 731.

## Controlling Degradation of Hydrogels via the Size of Cross-Linked Junctions

By Hyun Joon Kong, Eben Alsberg, Darnell Kaigler, Kuen Yong Lee, and David J. Mooney\*

Hydrogels are being increasingly called upon to perform complex functions in biological applications.<sup>[1]</sup> Their assistance in fulfilling these roles is frequently hypothesized to depend upon their playing a temporarily dynamic role via controlled degradation.<sup>[2]</sup> A variety of hydrogel systems prepared with degradable polymers have been previously developed (e.g., poly(lactide) and its derivatives,<sup>[3,4]</sup> hyaluronic acid,<sup>[5]</sup> gelatin,<sup>[6]</sup> or polymers modified to be labile to hydrolysis,<sup>[7]</sup> gels crosslinked with enzymatically labile molecules<sup>[8]</sup>), in which the degradation rate is mainly regulated by various intrinsic and extrinsic chemical factors. However, controlling material degradation via a simple physical dissociation of polymer molecules may provide advantages over chemical degradation. In this report, we introduce a new approach to regulate the degradation kinetics of ionically crosslinked gels via controlling the dissociation rate of the polymer chains. We also demonstrate the importance of controlling the degradation of these hydrogels to the formation of cartilage tissues that result from cell transplantation.

To investigate whether the degradation rate of hydrogels could be regulated by the dissociation of ionically crosslinked

polymer chains, we hypothesized that controlling the size mismatch between polymer segments that control ionic cross-linking would modulate the dissociation rate of polymers. To test this hypothesis, calcium-crosslinked alginate hydrogels consisting of alginates having different molecular weights ( $MW$ s) were used, and the molecular weight of the guluronic acid (G) blocks ( $MW_G$ ) in the polymer chains was varied in order to alter the size of the polymer segments responsible for ionic cross linking.<sup>[9]</sup> Specifically, high- $MW$  alginate rich in G blocks (MVG;  $MW \sim 269\,100\text{ g mol}^{-1}$ ), high- $MW$  alginate rich in mannuronic acid (M) blocks (MVM;  $MW \sim 280\,000\text{ g mol}^{-1}$ ), and low- $MW$  MVG ( $MW \sim 53\,100\text{ g mol}^{-1}$ ) rich in G blocks were used in these studies in order to differentiate between the effects of the overall polymer chain  $MW$  and effects of  $MW_G$ . Measurement of  $MW_G$  following isolation of G blocks from the various alginates showed that G blocks in the MVG polymer ( $MW_G \sim 5540\text{ g mol}^{-1}$ ) were  $1.5 \times$  longer than those in MVM ( $MW_G \sim 3640\text{ g mol}^{-1}$ ). The low  $MW$  MVG, prepared by irradiating MVG with  $\gamma$ -rays, maintained the  $MW_G$  of MVG ( $MW_G \sim 4960\text{ g mol}^{-1}$ ).

Six different gels were prepared from the different alginates. The gels were comprised solely of each of the high and low- $MW$  polymers (unary MVG, unary MVM, and unary low  $MW$  MVG gels), a gel formed from a combination of MVG and low- $MW$  MVG (binary MVG gel)<sup>[10]</sup>, a gel from MVM and low- $MW$  MVG (binary MVM gel I), and a gel from MVM and MVG (binary MVM gel II). The latter two gels exhibited size mismatch between  $MW_G$ , whilst the remaining gels exhibited a similar  $MW_G$  between the chains forming the gels, even though the polymer chain  $MW$ s were varied.

The initial physical properties of the varying hydrogels were quantified with the compressive elastic moduli ( $E$ ) and swelling ratios ( $Q$ ) of the gels. The physical properties of these were greatly dependent upon  $MW_G$ , but only weakly dependent on  $MW$  (Table 1). Thus, a lower  $E$  value was calculated for unary MVM gels and a higher  $Q$  value than both high- $MW$  MVG and low- $MW$  MVG gels. In contrast, the  $E$  and  $Q$  values of unary low- $MW$  MVG gels and binary MVG gels

**Table 1.** Compressive elastic modulus ( $E$ ) and swelling ratio ( $Q$ ) of the 5 wt.-% gels used in studies. The weight fraction of high- $MW$  ( $W(\text{high } MW)$ ) and low- $MW$  ( $W(\text{low } MW)$ ) polymer, containing either a high (MVG) or low fraction of G blocks (MVM), are indicated for each gel type.

Hydrogels	$W(\text{High } MW)$	$W(\text{Low } MW)$	$E$ [kPa]	$Q$
Unary MVG	1.0	0	$135 \pm 11$	$16 \pm 0.5$
Unary low $MW$ MVG	0	1.0	$110 \pm 9$	$19 \pm 2$
Binary MVG	0.5	0.5	$130 \pm 10$	$20 \pm 0.3$
Unary MVM	1.0	0	$54 \pm 6$	$25 \pm 0.6$
Binary MVM I	0.5	0.5	$90 \pm 4$	$22 \pm 0.1$

were comparable to those of unary MVG gels. This was likely due to the comparable  $MW_G$  of alginate chains. In the same context, binary MVM gel I had a significantly increased value of  $E$ , as compared to unary MVM gels.

[\*] Prof. D. J. Mooney, Dr. H. J. Kong  
Division of Engineering and Applied Sciences  
Harvard University  
Cambridge, MA 02138 (USA)  
E-mail: mooneyd@deas.harvard.edu

Dr. E. Alsberg  
Biomedical Engineering Department  
University of Michigan  
2200 Bonisteel Avenue, Ann Arbor, MI 48109 (USA)

Dr. D. Kaigler  
Department of Biological and Material Sciences  
Dentistry, University of Michigan  
Ann Arbor, MI 48109 (USA)

Prof. K. Y. Lee  
College of Chemical Engineering, Hanyang University,  
Seoul 133-791 (South Korea)